Chemistry Europe
European Chemical Societies Publishing

WILEY VCH

Excellence in Chemistry Research

Announcing our new flagship journal

- Gold Open Access
- Publishing charges waived
- Preprints welcome
- Edited by active scientists

Meet the Editors of *ChemistryEurope*

Luisa De Cola
Università degli Studi di Milano Statale, Italy

Ive Hermans
University of Wisconsin-Madison, USA

Ken Tanaka
Tokyo Institute of Technology, Japan

CHEMPHYSCHEM
REVIEWS

ChemPubSoc Europe

DOI: 10.1002/cphc.201402195

Thermodynamic and Mechanical Timescales Involved in Foam Film Rupture and Liquid Foam Coalescence

Emmanuelle Rio[a] and Anne-Laure Biance*[b]

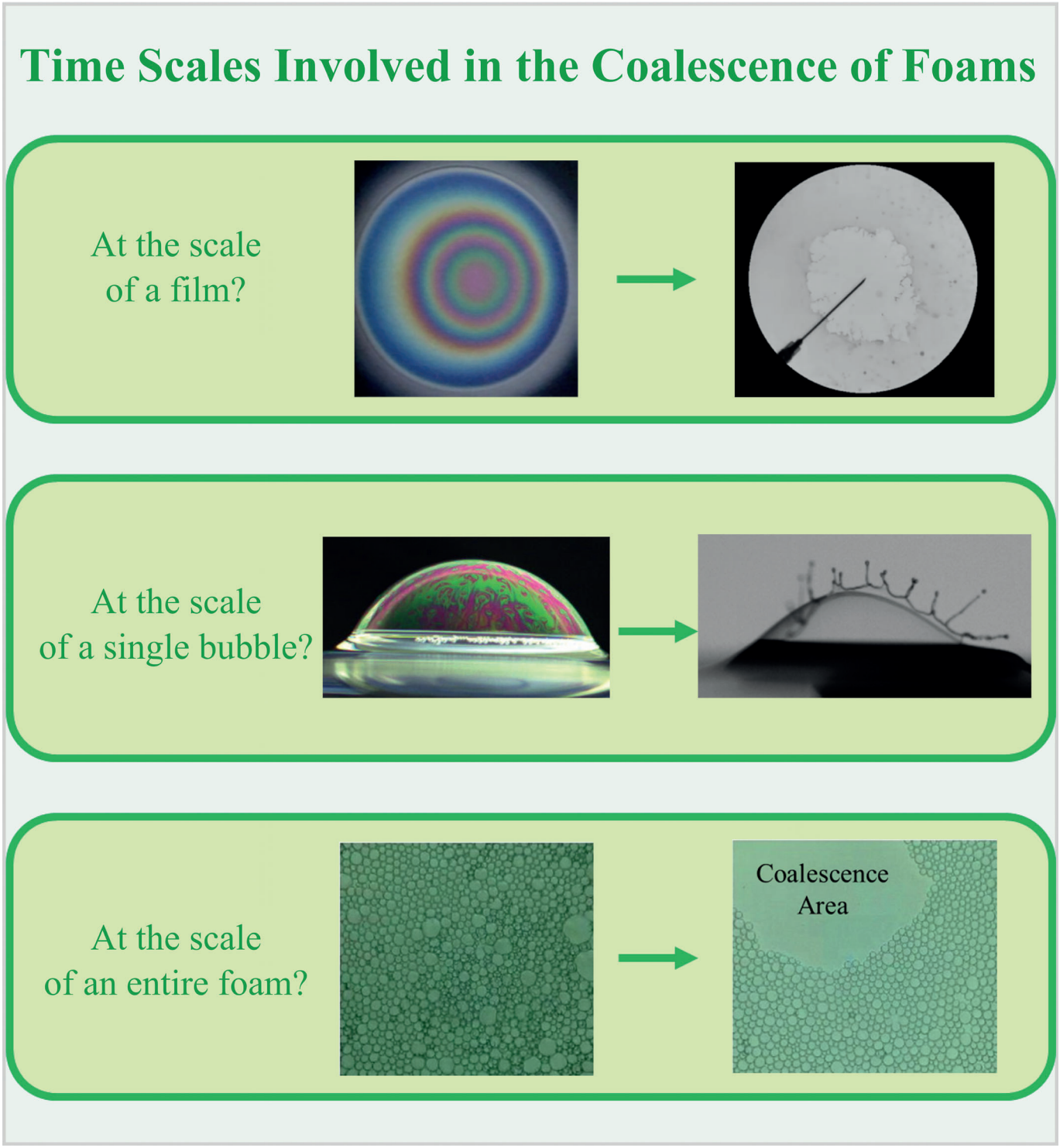

Recent advances in the coalescence in liquid foams are reviewed, with a special focus on the multiscale structure of foams. Studies concerning the stability of isolated foam films, on the one hand, and the coalescence process in macroscopic foams, on the other hand, are not always in good agreement. This discrepancy reveals that two routes can induce coalescence in a foam. The first route is thermodynamic and shows that coalescence is governed by a stochastic rupture of foam films. The second route relies on a mechanically induced rupture of the films, due to the spontaneous evolution of foams. From a literature review, the evaluation of the different timescales involved in these mechanisms allows defining the limiting parameters of foam coalescence.

1. Introduction

Liquid foams are widely encountered in everyday life as well as in industry,[1] and their stability is crucial for many aspects of their use. For example, one can desire a stable foam to prepare a chocolate cream or become exasperated when faced with a very stable foam while emptying a bathtub or a sink. Unfortunately, the important question "How long will this foam last?" has yet to be answered.

Different mechanisms, such as coarsening, drainage, or coalescence are at the origin of foam destabilization and bubble disappearance. Among them, coalescence, which corresponds to the merging of two bubbles, because of film rupture, is still poorly understood, because it is difficult to probe experimentally and appears to depend on many different factors, as shown herein.

One of the difficulties encountered in linking microscopic and macroscopic properties of foams is the existence of many length scales (Figure 1). The foam is a macroscopic product, the size of which can range from centimeters in cosmetics to meters in nuclear decontamination or in oil recovery. Among these length scales, the bubble size, R_v, is defined by the radius of a spherical bubble of an equivalent volume, the size of which varies between 1 cm and 10 μm. Two bubbles are separated by a film of thickness h, of less than 10 μm. Three films join in a small channel called a plateau border (PB) that contains most of the liquid of the foam. The plateau border length ℓ is close to the bubble radius R_v whereas its section scales with r^2, where r is the radius of curvature of the PB. Four PBs meet in a node, the volume of which is proportional to r^3. Lastly, foams cannot be stabilized without surface active materials, which are often of subnanometer dimensions.

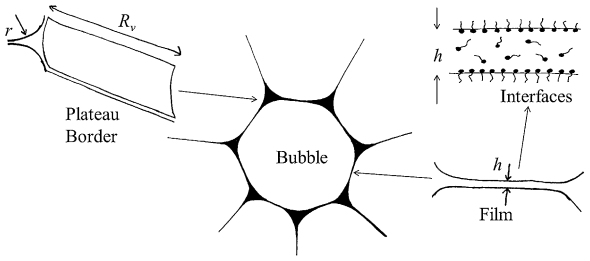

Figure 1. Multiscale description of a foam. Bubbles are dispersed in the liquid phase. They are separated by films of thickness h, the interfaces of which are covered by surfactants. Three films meet in a plateau border of length ℓ and section r^2.

A crucial parameter that has been shown to govern foam stability is the liquid fraction of the foam, noted Φ, which is defined as the ratio of the liquid volume V_{liq} to the foam volume V. We consider here only the case of foams in which the bubbles are in contact with one another, in contrast to bubbly liquids in which the bubbles are well-separated and remain spherical. Depending on the organization of the bubbles, the critical liquid fraction under which the bubbles come into contact lies between $\Phi_c = 0.26$ for ordered monodisperse bubbles, and $\Phi_c = 0.36$ for reasonably monodisperse, randomly packed bubbles. For smaller liquid fractions, most of the liquid is assumed to be contained in the PBs, so the liquid fraction is fixed by the ratio between the volume of the PBs ($V_{PB} \propto r^2 R_v$) and the volume of the bubble ($V_B \propto R_v^3$), given by Equation (1):

$$\Phi \approx \frac{r^2}{R_v^2} \tag{1}$$

Note that this relationship is valid only for foams with intermediate liquid fractions around 0.01. Nodes should be taken into account for larger liquid fractions[2] and film contributions are important at lower liquid fractions ($\phi \ll 0.001$).[3]

As shown by Equation (1), the quantity of liquid in a foam is a crucial parameter because it fixes the radius of curvature of the plateau borders. The capillary pressure P_c, that is, the pressure difference between the liquid inside the plateau borders and the air inside a bubble, sets the force applied to the bubbles and is given by Equation (2):

$$P_c \approx \frac{\gamma}{r} \approx \frac{\gamma}{R_v \sqrt{\phi}} \tag{2}$$

in which γ is the surface tension. To increase the complexity, different dynamic processes play a role at each scale of the foam. Surfactants adsorb and desorb from the interface and have a particular mobility in the bulk and at the interface. The drainage (liquid flow) in films differs from the drainage in PBs

[a] *Dr. E. Rio*
Laboratoire de Physique des Solides
Université Paris Sud-CNRS
UMR8502, Bat 510
91405 Orsay cedex (France)

[b] *Dr. A.-L. Biance*
Institut Lumière Matière
University Lyon 1-CNRS
UMR 5306, Université de Lyon
69622 Villeurbanne cedex (France)
E-mail: anne-laure.biance@univ-lyon1.fr

and from bubble coarsening (flow of gas between bubbles), with a strong interplay between all these mechanisms of foam evolution.[4]

Coalescence, on which we focus herein, is, by definition (from the Latin word *coalescere*—to grow), the merging of two bubbles to make a larger one, implying the rupture of the contacting film between the two bubbles. As shown by two recent reviews on the subject,[5,6] it is possible to benefit from the multiscale structure of the foam to describe the coalescence process. In the first review,[5] the main claim is that coalescence occurs because of dynamic events, which are easily triggered below a critical liquid fraction, whereas in the second review[6] the importance of the chemistry of the surface active agent is emphasized. Rio and Langevin describe the different reported mechanisms including a mechanism of coalescence at a critical bubble size.

In the present work, we introduce new results on the subject and compare both mechanisms to define a characteristic time of coalescence. It is then crucial not only to understand the origin of coalescence but also to define the relevant timescale at which it occurs and to compare it to other phenomena leading to the destruction of the foam. The very first question is whether such a timescale differential exists.

Coalescence might have two main origins: it can be triggered by mechanical solicitations or by thermodynamic fluctuations, leading, respectively, to a determinist or a stochastic rupture time. Our goal, based on a literature review, is to list the mechanisms at play at each length scale of the foam and to extract the characteristic timescales; these timescales depend on the mechanical properties of the interfaces and they are tuned by the surfactant chemistry. We chose to work with a standard foam throughout the paper to evaluate the orders of magnitude of these timescales. Note that the lengths we chose are for illustration and can vary by orders of magnitude from one foam to the other. Let us assume the initial thickness of the film to be $h \simeq 1\ \mu m$ and its typical radius (close to the bubble radius) to be $R_v \simeq 50\ \mu m$. The PBs have a radius of curvature $r = 6\ \mu m$, which corresponds to a liquid fraction of 0.5%. The surfactant solution is an aqueous surfactant solution of viscosity $\eta = 10^{-3}$ Pa s, density $\rho = 1000\ kg\,m^{-3}$ and surface tension $\gamma = 35\ mN\,m^{-1}$.

In the Section 2, we describe the stability of isolated films. We show that their bursting occurs in four steps. The film first thins and might reach a stable thickness. Instabilities then develop, allowing the local appearance of a bare interface, in which a hole can nucleate and invade the whole film. We extract the characteristic timescales for these different steps and show that, depending on the situation, the film rupture can be set by either drainage or fluctuations.

In Section 3, we focus on the rupture of isolated films or bubbles subjected to well-defined deformations. We show that many mechanical forces that may occur in foams due to aging or flow can induce coalescence. This emphasizes the importance of external solicitations such as shear. We extract the characteristic timescale for rupture events inside the foam.

In Section 4, we review the literature on 3D foams. We show that two opposite mechanisms, which are based on the existence of a critical liquid fraction or of a critical capillary pressure, are proposed. We review the arguments in favor of each mechanism and show that a lack of data prevents a clear conclusion. Finally, we attempt to compare the characteristic timescales extracted at each scale in the two limits of rigid and mobile interfaces and, provided that the coarsening is not too fast, we show that the drainage of the foam is certainly the most important time value with which to predict how long a foam will last.

Dr. E. Rio received her Master's degree. from École Supérieure de Physique et de Chimie Industrielles (ESPCI) and University Paris 6 (France) in 2002, and her Ph.D. from the same university in 2005 with Dr. L. Limat. After postdoctoral research in the laboratory of Prof. T. Bohr (Technical University of Denmark, Denmark), she accepted a position as Assistant Professor at the University of Paris Sud 11 in 2006. Her research interests include foams stability

Dr. A-L Biance received her Master's degree from École Supérieure de Physique et de Chimie Industrielles (ESPCI) and University Paris 6 (France) in 2001, and her Ph.D. from the same university in 2004 with Prof. D. Quéré. After postdoctoral research in the laboratory of Prof. L. Auvray (University of Evry, France), she accepted a position as a CNRS research scientist at the University of Marne La Vallée in 2006. She joined the University of Lyon in 2009.

2. Stability of Isolated Foam Films

Coalescence mechanism implies the rupture of one single film. To rupture, the film thins under capillary suction or gravity-driven drainage. In the absence of repulsion between both interfaces, the film is unstable and reaches a critical thickness at which the development of an instability triggers immediate rupture. The time necessary to rupture the film is expected to be the sum of the characteristic times of the different processes involved: drainage, initiation of a rupture, and bursting process.

2.1. Film Drainage and Timescale Required to Reach a Specific Film Thickness

The drainage of a thin film results from liquid flow between two liquid/air interfaces. Precise experiments using interferometric probes to examine film thickness have been performed in Sheludko cells,[7] and extended modeling has been achieved

in different limiting cases. The goal of this section is to extract a characteristic drainage time.

The first step of a description of liquid flow during drainage is the conservation of momentum. In the case of thin films, in the lubrication approximation, this reduces to Equation (3):

$$\rho\frac{\partial\vec{v}}{\partial t}=\eta\vec{\Delta}\vec{v}-\vec{\nabla}P+\rho\vec{g} \tag{3}$$

where $\vec{v}$ is the liquid velocity, $\vec{g}$ is the gravitational acceleration, and P is the pressure field. P contains the capillary pressure $P_c \cong -\gamma\frac{\partial^2 h}{\partial x^2}$ (see Figure 2 for notations).

To this equation is associated a mass conservation that links the flow velocity and the evolution of the film thickness [Eq. (4)]:

$$\frac{\partial h}{\partial t}+\frac{\partial hv}{\partial x}=0 \tag{4}$$

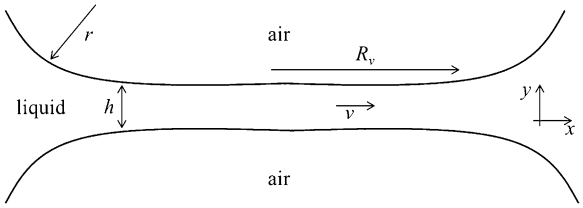

Figure 2. Drainage of a thin film under capillary suction.

These equations must be completed by an appropriate boundary condition at the liquid/air interface, which is crucial to determine properly the drainage dynamics, as observed by Mysels,[8] who studied the drainage of a foam film under gravity. He observed two limiting cases of drainage, depending on whether the surfactant induces mobile or rigid interfaces. This terminology fixes the limit boundary condition at the liquid/air interface: zero velocity at a rigid interface and zero stress at a mobile interface. For intermediate cases, the complete set of boundary conditions requires a stress balance and takes into account surfactant presence and nature, which can be combined in Equation (5)[9,10] (in two dimensions and in the lubrication approximation):

$$\eta\frac{\partial v}{\partial y}=\frac{\partial\gamma}{\partial x}+\eta_s\frac{\partial^2 u_s}{\partial x^2} \tag{5}$$

where u_s is the surface velocity and η_s is the surface viscosity (a combination of shear and dilatational viscosity that takes into account the deformation of the surface).[11] These equations must be completed by linking microscopic characteristics and mechanical properties of the interface. Local surface tension can be related to local surfactant concentration by thermodynamic relationships.[12] Exchange between surface and bulk are described by a combination of a thermodynamic equilibrium and of adsorption and desorption mechanisms.[13] The mass transport of the surfactants along the interface and in the bulk is described by relationships of mass conservation given by Equations (6) and (7):

$$\frac{\partial\Gamma}{\partial t}+\vec{\nabla}(\Gamma\vec{v}_s)-D_s\Delta_s\Gamma=j \tag{6}$$

$$\frac{\partial c}{\partial t}+\vec{\nabla}(\vec{v}c)-D\Delta c=0 \tag{7}$$

where c is the bulk and Γ is the surface concentration of the surfactants, D and D_s are bulk and surface diffusion coefficients, respectively, v_s is the surface velocity; and j is a source term describing adsorption and desorption of the surfactants.

A first level of description is to consider a quasistationary flow in a flat, nondeformable, film. If the boundary condition is simply taken as a zero velocity at the interface, this leads to the Reynolds velocity,[14] which reads as Equation (8):

$$V_{\mathrm{Re}}=\frac{2\gamma h^3}{3\eta R_v^2 r} \tag{8}$$

in the case of capillary drainage. Sonin et al.[15] consider also this flat film hypothesis but take into account a more complex boundary condition by using Equation (5). They neglect the diffusion of surfactants along the interface and in the bulk, as well as the surface viscosity. A reasonable agreement with experimental measurements of the thickness at the center of the film was found (nonionic surfactants below the cmc).

The case of deformable interfaces is more complex. It was solved analytically with the assumption of a rigid interface (zero velocity at the interface) by Aradian et al.[16] by applying an asymptotic matching technique. Howell and Stone[17] considered the case of surfactant-free interfaces (stress-free interfaces) and determined a drainage time for this fast limit. In the presence of such deformable interfaces, a dimple can appear in the middle of the film (Figure 3).

As regards experimental work, the drainage between two microbubbles approaching each other with a controlled force monitored by AFM was studied.[18] The effect of surfactants was taken into account by numerical modeling of the drainage[19] in the insoluble limit, without surface viscosity. A quantitative agreement between experiments and analysis was ob-

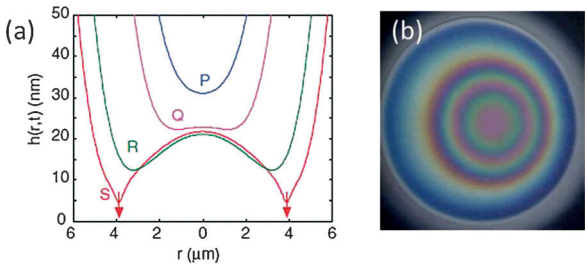

Figure 3. a) A dimple with rigid interfaces obtained by using lubrication theory in the presence of Van der Waals attraction. Reprinted with permission from Ref. [95]. Copyright 2010 High Wire Press. b) Photograph of a dimple during the thinning of a film obtained with a mixed solution, with applied pressure 100 Pa [polyacrylamide sulfonate (PAMPS) and dodecyl β-glucoside]. Image courtesy of D. Langevin and J. Delacotte.

served. From these studies, we can deduce that the film drainage should depend on many parameters.

As a limiting case, one can consider either rigid or mobile deformable interfaces. In the rigid case, a characteristic timescale shown in Equation (9) can be extracted from the model of Aradian et al.:[16]

$$\tau_{Ar} = \frac{3\eta r^2}{4\gamma h} \quad (9)$$

leading to $\tau_{Ar}^{(1)} \simeq 8$ μs to reach 100 nm and $\tau_{Ar}^{(2)} \simeq 80$ μs to reach 10 nm for a film of the model foam presented in the Introduction. Another timescale can be derived in the mobile limit as defined by Howell and Stone.[17] The obtained characteristic time t_{Ho}, which does not depend on film thickness, is given by Equation (10):

$$t_{Ho} = \frac{4\eta r}{\gamma} \cong 0.7\ \mu s \quad (10)$$

The transition between these two regimes[20] can be determined by considering the dimensionless Marangoni (*Ma*) and Boussinesq (*Bq*) numbers, which compare, respectively, the Marangoni or the surface viscosity effects to the bulk viscous stress. These numbers are given by Equation (11):

$$Bq = \frac{\eta_s}{R_v \eta} \quad (11)$$

and Equation (12):

$$Ma = \frac{\Delta\gamma}{\eta v}, \quad (12)$$

with $\Delta\gamma$ being the typical variation of surface tension along the interface. If one of these numbers is large, the limit of almost rigid interfaces should be considered, whereas if they are both small, the mobile limit should apply.

As a conclusion, we identify a characteristic drainage time for the rigid [Eq. (9)] and the mobile limits [Eq. (10)]. They can differ by several orders of magnitude. In Section 2.2, we will explore the other characteristic timescales implied in film rupture.

2.2. Timescale to Initiate Rupture

We consider here the time necessary to initiate a hole in a foam film, once the film has thinned. One crucial factor to determine whether a film is stable or not, is its thickness.[21–23] Let us define a number of notations. The equilibrium thickness at which the film thickness stabilizes and stops thinning is denoted h_{eq}. The thickness below which an instability starts to develop leading to the rupture of the film is referred to as the stability thickness, noted h_{st}. Lastly, we call the thickness at which the film actually ruptures, the *bursting* thickness h_{br}. Depending on the scenario considered, h_{br} can be equal to h_{st}, to h_{eq} or can have a different value.

2.2.1. Thickness h_{eq} of a Foam Film at Equilibrium and Shape of the Disjoining Pressure Curve

A film of pure liquid surrounded by air is not stable because of the nature of Van der Waals attractive interactions on both sides of the film.[24] To stabilize it, the presence of surfactants at the interface is mandatory to generate steric and electrostatic repulsion. As summarized in Figure 4, the different interactions (attractive Van der Waals interactions, electrostatic, and steric repulsions) allow, for a given disjoining pressure, two metastable states to be defined corresponding to two local minima of energy. The one with the larger thickness h_2 gives rise to so-called Common Black Films (CBFs), stabilized by electrostatic forces. The state defined by the smaller thickness h_1 corresponds to Newton Black Films (NBFs).

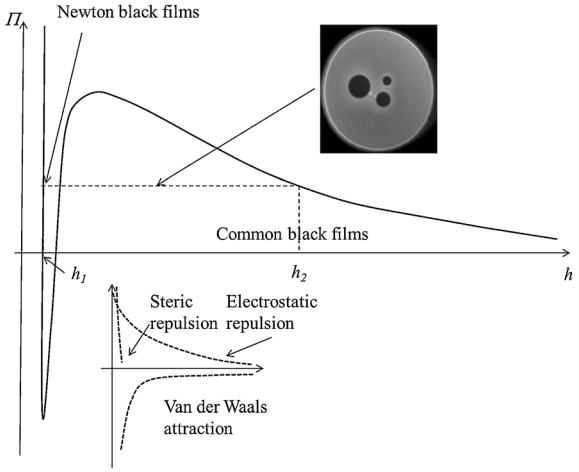

Figure 4. A typical curve for disjoining pressure versus film thickness *h*. CBF corresponds to a thickness h_2, whereas NBF exhibits a thickness h_1. The transition between both states is observed through spinodal decomposition (see image). Inset: contribution of steric, electrostatic and Van der Waals interactions. Adapted from Ref. [24] with permission. Photograph: picture of the opening of a thinner film inside a thicker one. The black spots are thinner domains and expand during the spinodal decomposition.

Many measurements have been performed and reported in the literature (see Ref. [25] and references therein) measuring $\Pi(h)$ curves on foam films, varying the surfactant nature and concentration, the salt content,[26] or adding polymers.[27] The most widely used experimental system is the thin-film pressure balance apparatus, first developed by Sheludko[7] and by Mysels and Jones,[28] that allows the disjoining pressure to be balanced by an applied controlled pressure. Reasonable agreement with the Derjaguin and Landau, Verwey, and Overbeek (DLVO) theory has been observed.

If the pressure is smaller than the local maximum, two branches of the disjoining pressure curves are stable; these correspond to the NBFs (thicknesses below 5 nm) and to the CBFs (thicknesses in the range 10–100 nm) described above. If the pressure is larger than this critical pressure, CBFs no longer exist.[29] In a macroscopic foam, the liquid fraction sets the capillary pressure, which is balanced by the disjoining pressure.

The thickness of the film can then be deduced from the curve $\Pi(h)$.

2.2.2. Role of Thermal Fluctuations in Film Rupture

In the absence of fluctuations, a film stabilized by surfactants is expected to be in a metastable state with a thickness determined by the disjoining pressure. However, observation shows that films eventually rupture even if great care is taken in experiments[7, 25, 29] to avoid external factors of rupture (e.g. evaporation or mechanical noise). Under these conditions, spontaneous thermal fluctuations are very likely to cause film rupture. Here, we consider the role of these fluctuations in the rupture of a bare film. We then explore the role of the surfactants on these fluctuations and on the stability of the films. Finally, we discuss the timescales involved and the conditions for the stochastic rupture of the films.

2.2.2.1. Rupture of a Bare Thin Liquid Film: Existence of h_{st}

A hole destabilizes a liquid film only if its width is larger than the film thickness.[30] Consequently, the activation energy to create a destabilizing hole scales as γh^2. If compared to the thermal energy kT, a stability thickness at which the liquid film is unstable can be defined and is of the order of 1 nm,[31] far below the experimental observations mentioned above. Then not only the activation energy must be taken into account, but also thermal fluctuations. Thermal corrugations of the interface (Figure 5 a) of thin liquid films were first observed by light-scattering experiments.[32] These fluctuations, which are inhibited by surface tension, are enhanced by Van der Waals attractive interactions between both sides of the film. Then, by taking into account both effects, Vrij and Overbeek[33] determine the critical wavelength Λ_c of the thermal fluctuations that are amplified; this led to Equation (13):

$$\Lambda_c = 2\pi\sqrt{\frac{\pi\gamma h^4}{A}} \tag{13}$$

where A is the Hamaker constant. The cheapest fluctuation in terms of energetic cost is that with the largest wavelength; this sets a relationship between a critical thickness h_{st} at which the film ruptures and the lateral size of the film [Eq. (13) with $h = h_{st}$], predicting that larger films are less stable. Vrij also proposes a time for a fluctuation to develop in such a stationary film [Eq. (14)]:[34]

$$t_{br}^{(1)} = 10^{*}96\pi^2\eta\gamma A^{-2}h_{st}^5 \tag{14}$$

where $A \simeq 10^{-20}$ J. This bursting time depends dramatically on the film thickness, and we estimate $t_{br}^{(1)} \simeq 330$ ms for $h = 10$ nm and $t_{br}^{(1)} \simeq 10^3$ s for $h = 50$ nm. At small thicknesses (i.e. when h_{eq} is small), this time is comparable to draining times calculated in the Section 2.1, whereas at large thicknesses (large h_{eq}), it will be much larger and it will be the limiting time in the rupture of the film. Concerning rupture in dynamic conditions, during drainage, Vrij[34] also proposes that the film ruptures at a critical thickness obtained by minimizing the sum of the draining time and of the time for an instability to establish itself. Let us recall that these models, which include a destabilizing Van der Waals attraction at short distance, apply only in the presence of bare interfaces.

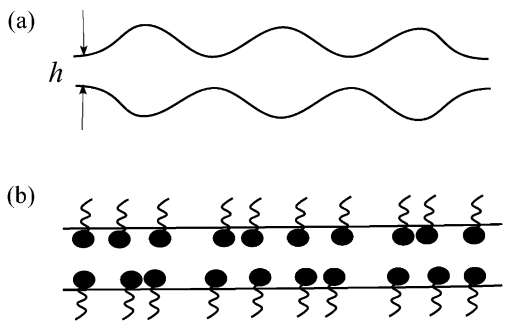

Figure 5. a) Corrugations and b) surface concentration fluctuations at the interfaces of a foam film.

2.2.2.2. Role of Surfactants

The inclusion of surfactants leads to short-range repulsive interactions, which limits film rupture, but this effect is not sufficient to stabilize foam films. The presence of surfactants has other consequences on thin liquid film stability, which is enhanced by several mechanisms: 1) the surfactants counteract the attractive Van der Waals interaction by damping or limiting the fluctuations, 2) they are at the origin of a bending energy, which must be overcome.

- Thickness fluctuations damping: Energetic cost associated with thermal fluctuations is increased by the elasticity of the surfactant layer.[29] This effect tends to decrease the probability of spatial fluctuations. For very rigid films, the surface elastic modulus E can exceed the surface tension and this governs the probability of expansion of a fluctuation. This effect is the common mechanism, named Gibbs–Maragoni effect, describing how the presence of surfactants can increase thin-film stability.[13]
- Curvature energy associated with hole nucleation: The large curvature energy interfaces covered by surfactants is also a stabilizing effect of thin liquid films.[35] Indeed, the nucleation of a hole in a thin film is associated with a large curvature (the radius of which is equal to the film thickness), which has an energetic cost that increases the energetic barrier to overcome for rupture. This energy is larger when the size of the hydrophilic head of the surfactant is increased. The curvature energy is nevertheless very small for most common surfactants and becomes negligible as soon as the surface tension is large enough, which is very often the case in foams.

Besides these different stabilizing effects of the presence of surfactant, different mechanisms for foam film rupture have been proposed, although there is a very large short-range repulsive force between interfaces. They all rely on stochastic

energy wherein thermal fluctuations are the key ingredient inducing film rupture.

The first mechanism considers that the film is likely to rupture if a bare zone appears on the foam film. Such a zone is likely to appear if fluctuations in the surface concentration of surfactants[21] are present (see in Figure 5b). Similarly to the fluctuations of density that occur in a bulk material, fluctuations of surfactant coverage can occur at the interface of the film. The Gibbs modulus is then equivalent to the inverse of the bulk material compressibility. Then, the probability to form a bare zone of size h decreases when the Gibbs modulus increases.

Another mechanism has been proposed by Bergeron.[29] He suggests that fluctuations do not directly induce film rupture but that they decrease the barrier between CBF and NBF (Figure 4). Then CBFs become thin NBFs, which can be destabilized by one of the mechanisms described above. The appearance of a bare zone in a NBF very probably entails film rupture because it is thin and likely to burst [bursting time proportional to h^5 in Eq. (14)]. This could explain why in many experimental studies rupture times have been shown to be independent of the disjoining pressure curve[25,29,36] and also why surface elasticity is often invoked to explain film stability even if no clear correlation between both can be exhibited.[29,36]

2.2.2.3. Conditions for Film Rupture

In all the descriptions mentioned above, film rupture is a stochastic process induced by thermal activation. The probability P for rupture is then given by Equation (15):

$$P \approx cexp(-\frac{\Delta G_s}{kT}) \quad (15)$$

with c being a constant allowing a normalized probability, ΔG_s the energetic barrier, and kT the thermal energy. The time for rupture is expected to be proportional to $1/P$, leading to Equation (16):

$$t_{br}^{(2)} \cong \tau_0 \exp(\frac{\Delta G_s}{kT}) \quad (16)$$

When surface elastic modulus is small, ΔG_s is also small and rupture is almost determinist with $t_{br}^{(2)} \approx \tau_0$. If we assume that τ_0 is the time for a molecule to diffuse over a typical length ℓ given by the distance between surfactants $\ell^2 \approx 50$ Å^2 and that the diffusion coefficient is given by the Einstein law $D = \frac{kT}{6\pi\eta\ell}$ then Equation (17) is obtained:

$$t_{br}^{(2)} \cong \tau_0 = \frac{6\pi\eta\ell^3}{kT} \cong 1.6.10^{-9}\text{s} \quad (17)$$

When the surface elastic modulus is larger, the fluctuations of the surfactant concentration become relevant. We can consider that the interface becomes unstable as soon as a bare interface of size close to h is created (the situation is then close to that of a bare film). The energy barrier to overcome is then equal to Eh^2.[30,37] The time for rupture scales as the inverse of this probability, given in Equation (18):

$$\frac{\Delta G_s}{kT} = \frac{Eh^2}{kT} \approx 700 \quad (18)$$

taking a typical value of 30 mN m^{-1} for E and a film thickness of 10 nm. Estimation results in gigantic values of $t_{br}^{(2)}$, which led de Gennes to say that a foam film should never burst in the absence of impurities.[38] If elasticity reaches a small value around 0.5 mN m^{-1}, which is small but not unrealistic, the time can then reach 280 μs and be comparable to the draining time.

2.2.3. Three Scenarios for the Rupture of Thin Films at Rest

Finally, according to the literature, bursting requires different processes: the film drainage (see Section 2.1), the appearance of a bare zone, and the initiation of a hole. Depending on the scenario of rupture, these steps need to be fulfilled or not and have different timescales. To summarize, three cases can be considered.

The first is purely thermodynamics: the film reaches, through drainage, an equilibrium thickness h_{eq}. This thickness is well described by the interactions between the two interfaces of the film and by the DLVO theory[24] in the case of charged surfactants.[25] The liquid can include some impurities or some instabilities can develop and lead to rupture.[38] In this case, h_{br} is equal or close to h_{eq}. The rupture time after drainage is then the time for the instability to develop $t_{br}^{(2)}$ and to initiate a hole $t_{br}^{(1)}$.

The second scenario takes place if the capillary pressure[22,39] is above a critical value, allowing spinodal decomposition between two states of different film thicknesses (inset of Figure 4). This decomposition is only possible if the pressure applied is larger than a barrier that depends on the disjoining pressure in the film, as depicted in Figure 4. The film then ruptures because of instabilities that develop in its thinner part. In this case, the rupture time after drainage is the time necessary to overcome the disjoining pressure barrier at a given pressure plus the time necessary for the instability to develop. The total time is again the sum $t_{br}^{(2)} + t_{br}^{(1)}$.

The third rupture scenario relies on kinetic parameters: rupture takes place during drainage, when the film remains thick. A bursting thickness can then be defined at which instabilities lead to rupture. Roughly reproducible values of h_{br} have been measured and are well described by the disjoining pressure equation together with hydrodynamics.[22,23] The bursting thickness extracted from these references is around 30 nm, which is thicker than NBFs because the film bursts during drainage. The bursting time is then governed by the drainage time, given by Equation (10) and Equation (9). Manev et al.[40] develop a more sophisticated model with an influence of the drainage velocity on the bursting thickness.

Each scenario is then expected depending on the external parameters: A high velocity should lead to the third scenario, whereas a small external pressure applied should lead to scenario 1 and a large external pressure to scenario 2.

2.3. Timescale of Hole Opening

Once the characteristic time of drainage to reach an unstable configuration and the time to nucleate a hole in the film have elapsed, we face another timescale in foam coalescence and collapse, which is the time required for a hole to open. In the following, we discuss the different mechanisms of hole opening. Existing studies mainly concern the case of mobile films and in this simple case, at least two regimes can be identified. The first one at small Reynolds number $Re = \frac{\rho R_v v}{\eta}$ corresponds to a viscous regime, whereas the second one, which is more commonly observed for liquid in gas, corresponds to an inertial regime.

2.3.1. Inertial Regime

2.3.1.1. Mobile Surfaces

In the inertial regime, the dynamics of the hole opening results from a balance between surface tension and inertia. The first theoretical analysis of this regime dates back to Taylor,[30] who considered that the opening velocity of a hole in the film results from the dynamics of a rim (Figure 6) at the edge of the hole, which is given by Equation (19):

$$\frac{d}{dt}(mV) = 2\gamma \tag{19}$$

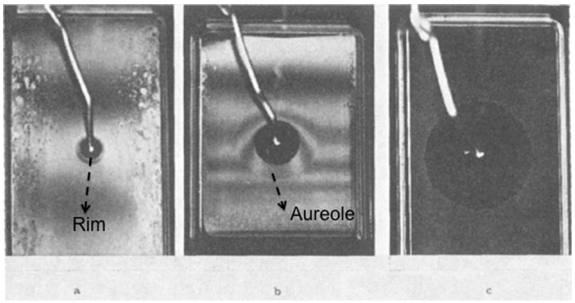

Figure 6. Different snapshots of hole-opening mechanisms. Differences between a rim and an aureole can be observed. From left to right, film thicknesses are 280, 430, and 10 nm. Reprinted with permission from Ref. [42]. Copyright 1969 American Chemical Society.

where m is the mass of the rim (varying with time as the rim swallows some part of the film as the hole increases) and V its velocity. Depending on the shape of the rim, this equation has a solution at constant velocity according to Equation (20):

$$V = \sqrt{\frac{\phi\gamma}{\rho h}} \tag{20}$$

where ϕ was demonstrated to be equal to two, one year later by Culick.[41] These results are in good agreement with stationary experiments performed on liquid sheets[30] and were extensively investigated by McEntee and Mysels in the case of foam films.[42] Snapshots of different regimes of hole opening are reported in Figure 6.

A timescale of hole opening can be defined in Equation (21):

$$\tau = \sqrt{\frac{\rho h R_v^2}{2\gamma}} \tag{21}$$

and is equal to 0.6 μs if the film bursts at a thickness of 10 nm.

2.3.1.2. Effect of Surface Elasticity

The effect of surface elasticity has been observed through the development of an aureole (Figure 6) around the opening hole. Different observations have been reported:

- The radius of this aureole expands with time and is attributed to the compression of the surfactants on the surface (at this timescale, surfactants do not have time to desorb). This aureole does not modify the Taylor–Culick prediction. The opening velocity of the hole is consistent with Equation (20), with ϕ slightly larger than 2. The shape and velocity field in this aureole follows a self-similar solution as described theoretically[43] and observed experimentally.[44]
- A deviation from this experimental law is observed for films thinner than 50 nm. This is attributed by Mysels[42] to modifications of the surface tension due to confinement. Another deviation at these film thicknesses has been attributed to the appearance of a bulk elasticity under confinement.[45]
- A second deviation from this law is observed for rigid films,[42] in which surface stress due to compression is too large and in which bending occurs. In this case, the opening velocity of the hole is one order of magnitude lower than expected. No systematic studies have been conducted to explore this effect.

As a conclusion, for mobile interfaces, Taylor–Culick law describes well the opening velocity of the hole, whereas for rigid interfaces (with rigidity being due to surfactant nature or confinement), discrepancies are reported. In both cases, the timescale of this process is of the order of a few microseconds.

2.3.2. Viscous Regime

When the viscosity in the film is increased, a viscous regime can be identified. The hole is surrounded by a rim, which expands at a constant velocity V. If we consider that the dissipation is located in the rim of height h, the stress balance scales as shown in Equation (22):[46]

$$\eta\frac{V}{h} \approx \frac{2\gamma}{h} \tag{22}$$

This results in a constant velocity that does not depend on the film thickness and reads $V = C\gamma/\eta$ with a constant C . In the case of a water film of thickness $h = 1$ μm, this velocity is larger than the Taylor–Culick velocity, underlying the conclusion that

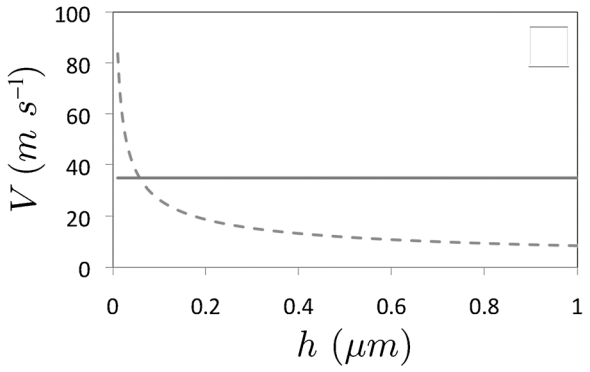

Figure 7. Dewetting velocity versus film thickness in inertial case (dashed line) according to Equation (20) and the viscous case (solid line) according to Equation (22). At low thicknesses, the viscous dissipation exceeds inertia, leading to a velocity smaller than the Taylor–Culick velocity. $\gamma = 35$ mN m^{-1}, $\eta = 0.001$ Pa s.

viscous dissipation is smaller than inertia. The dynamics will be then governed by the Taylor–Culick velocity. However, it appears to be dominant when the size of the film reaches the thickness h_v (Figure 7), at which the velocities given by Equation (20) and Equation (22) are equal [Eq. (23)]:

$$h_v = \frac{2\eta^2}{C^2\rho\gamma} \tag{23}$$

In the case of a foam film of surface tension 35 mN m^{-1}, this thickness is 57 nm. This could correspond to the discrepancies observed by Mysels for the thinner films.[42]

Other types of viscous bursting have been observed in the case of viscoelastic fluids such as highly viscous polydimethylsiloxane (PDMS) bubbles.[47] In this case, the development of the stress along the film appears at a velocity corresponding to the sound speed in the media, which is $\sqrt{E/\rho}$ if E is the elastic modulus of the media at high frequency. Then the subsequent viscous elongation is given by Equation (24):

$$\sigma_{r,r} = 2\eta\frac{\partial v}{\partial r} \tag{24}$$

where r is the radial coordinate. If this is balanced by the surface tension stress in the same direction $\approx \frac{2\gamma}{h}\left(\frac{R}{r}\right)^2$, the hole evolution follows an exponential increase as given by Equation (25):

$$R(t) = R_0 exp(\frac{\gamma t}{\eta h}) \tag{25}$$

In this case, the opening velocity of the hole depends on time and (if we consider that initial hole size is equal to the film thickness) is given by Equation (26):

$$V = \gamma/\eta exp(\gamma t/\eta h) \tag{26}$$

2.3.3. Fragmentation

During the rupture, the rim has been shown to destabilize into satellite droplets with a controlled size as shown in Figure 8. A flapping motion of the hole edge is observed, due to air friction, and the destabilization wavelength λ is set by a balance between surface tension and this friction and scales as: $\lambda \sim \gamma/\rho_{air}V^2$. No study has focused in detail on the size of the satellite droplets. If these droplets reach an adjacent film, they can trigger film rupture. If gravity is the main process for droplet ejection, the timescale for a droplet to reach adjacent films is given by $\tau_s = \sqrt{2R/g}$, which is of the order of 10 μs. Different processes can govern droplet ejection such as inertial entrainment, but these processes will be faster, showing that droplet ejection is not the limiting factor inducing film rupture.

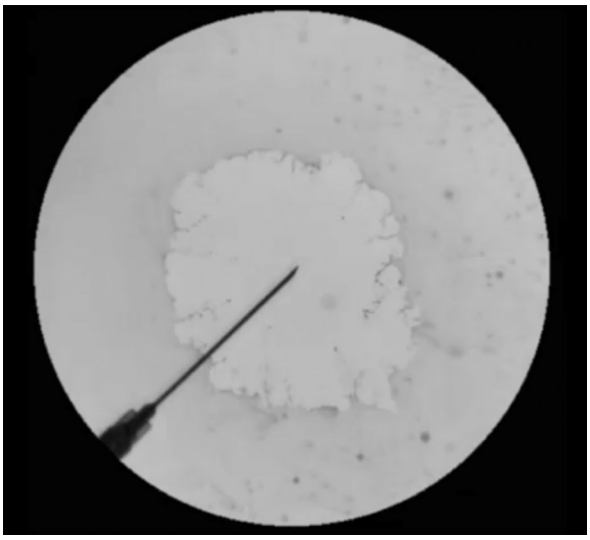

Figure 8. Image of the edge of a rupturing SDS foam film (frame size is 12 mm). Satellite droplets are observed from the edge of the hole.

2.4. Conclusion: Total Timescale for an Isolated Film to Burst

We list the following steps leading to film rupture, which are summarized in Table 1:

1. The film has an initial thickness h governed by external parameters and thins to reach the CBF thickness. If the interfaces are rigid, drainage lasts tens of microseconds, whereas for mobile interfaces it lasts tenths of microseconds [Eqs. (9) and (10)].
2. The second step is to overcome the barrier to the NBF. It lasts from hundreds of microseconds in the mobile limit to almost infinity in the rigid case [Eq. (16)]. Note that the film can also directly drain to a NBF. In this case, the second step does not exist.
3. An instability then develops for rupturing. A hypothetical scenario is that a thermally activated instability of characteristic time $t_{Br}^{(2)}$ that can also vary from a few hundred microseconds for mobile interfaces to almost infinity for rigid

Table 1. Timescales of isolated film rupture for our model film [$h=10$ nm, $R_v=50$ μm, $\eta=10^{-3}$ Pa s, $\gamma=35$ mN m, $\rho=1000$ kg m^{-3}] in the limit of mobile and rigid interfaces (defined in the text).

	Drainage	Instability $t_{br}^{(2)}$	Hole initiation $t_{br}^{(1)}$	Opening/ Fragmentation
Rigid	8–80 μs	>1 year	300 ms	0.6–10 μs
Mobile	0.7 μs	280 μs	300 ms	0.6–10 μs

ones [Eq. (16)] is followed by the appearance of a bare interface of size close to h. This bare interface destabilizes in a time fixed by Vrij $t_{Br}^{(1)} \approx 300$ ms.

4. Eventually, hole opening and the fragmentation take tenths of microseconds, which is negligible.

The total bursting time is the sum of all these timescales. Information that allows the determination of whether film rupture is stochastic or not can be gained by comparing the different durations. If the drainage time is larger than the time necessary to develop an instability, the rupture should be deterministic. In contrast, if the drainage time is smaller than the time necessary to develop an instability, then the rupture is expected to be stochastic. A quick look at Table 1 may lead the reader to think that the rupture is always stochastic because the drainage timescale is always shorter. Unfortunately, it is not clear that interfaces that can be considered as rigid for drainage can also be considered as rigid for the development of a given instability. It is thus possible to have timescales of drainage and of instability development very close to each other. We could then propose a dimensionless number comparing a deterministic time t_d due to drainage and a stochastic time t_s due to the development of instabilities, given by Equation (27):

$$DS = \frac{t_d}{t_s} \tag{27}$$

If DS is smaller than or close to one, the rupture will be stochastic, whereas if it is much larger than unity it will be deterministic. Note that another mechanism leading to a deterministic rupture time is the coupling of hydrodynamics and Van der Waals attraction as discussed in Section 2.2.3.[23]

3. Stability of Bubbles Subjected to Flow: Shear and Stretch

In this section, we consider situations in which foam films or bubble clusters undergo well-defined dynamic deformations. These deformations are considered in films, two bubble clusters, and 2D foams. Mechanisms leading to rupture in these specific situations are considered, and timescales of rupture can be compared to the imposed shear or elongation rate.

3.1. Stress on an Isolated Film Induces Its Rupture

It is commonly accepted that vertical foam films can resist gravity because of a surface tension gradient along their interfaces.[48] De Gennes proposed[38] a description of "young soap films" that would be generated very fast. Their shape and thickness is then expected to depend on thermodynamics, and the maximum length of a film pulled out from a bath is fixed by the maximum Marangoni gradient that can be established at the surface. Unfortunately, as noted by De Gennes, this description predicts very long films (tens of centimeters), which do not correspond to experimental observation. Another theoretical work performed on film drainage[49] shows numerically that when the film reaches a critical thickness, the surfactant flux necessary to compensate the stress induced by the drainage of the liquid on the surface diverges. This divergence is expected to account for rupture and takes place in films of 400 nm, leading to film lifetimes ranging between 10 and 100 s for various range of Ma numbers. These conclusions are more in line with experimental observations, although Common or Newton Black Films have been observed during drainage.

An experiment allowing film rupture in a dynamic situation to be observed was performed by Saulnier et al.[50,51] A foam film on a rigid frame was slowly withdrawn from a bath at a controlled velocity (ca. 1 mm s^{-1}) and a dependence of the film lifetime with respect to the pulling velocity was observed, as reported in Figure 9. The results show a systematic rupture of the film at a well-defined lifetime or film length, in contrast to experiments performed on horizontal films. If these results are interpreted by a stress balance between the weight of the film and a Marangoni stress at the interface, the difference of surface tension required has been shown to be very small (1–2 mN m^{-1} along the film).[51]

We will see in the following sections that other dynamic deformations of films/bubbles/foams have been reported as a mechanism that can be invoked to induce coalescence.

3.2. Coalescence due to Bubble Extension Deformation

It is commonly accepted that coalescence can be enhanced by shearing a foam; therefore, experiments aimed at understanding the mechanism of coalescence at the scale of a few bubbles under forced shear have been performed.[18,52–56] In each experiment, different mechanisms are proposed but, at this stage, the variation between the systems studied do not allow a generic picture of the coalescence process to be developed.

3.2.1. Two Bubbles/Drops

A number of different mechanical deformations have been investigated:

1. Competition between drainage and shear: Most experiments studying coalescence under mechanical deformations deal with droplet coalescence. However, considering the assumptions made in the mechanisms proposed for

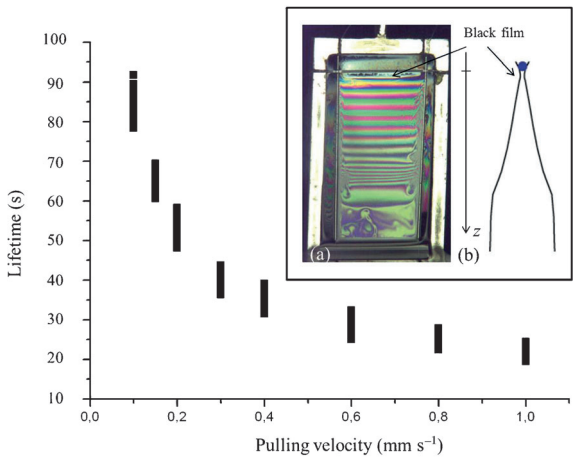

Figure 9. Lifetime of a film pulled out of a bath of soapy solution at a velocity *V*. Inset: a) Picture of a film during its generation together with b) a scheme of the film profile exhibiting a constant thickness at the bottom and a thinning zone at the top.

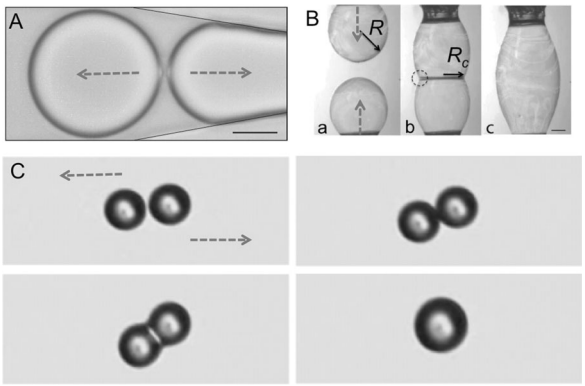

Figure 10. Different types of deformation induce coalescence: A) Coalescence of emulsion droplets, due to elongation and nipple formation. Reprinted with permission from Ref. [57]. Copyright 2008 American Physical Society. B) Noncoalescence and coalescence mechanism, due to the contact of two bubbles. Reprinted with permission from Ref. [56]. Copyright 2011 American Physical Society. C) Coalescence of two droplets during shear. Reprinted with permission from Ref. [53]. Copyright 2007 American Institute of Physics.

droplets, these results should be directly transposable to bubbles. Therefore, they are briefly discussed here along with experiments on bubbles.

Leal et al.[52,53] observed droplet coalescence under controlled shear (Figure 10C), created by four rotating cylinders. The droplets, which are covered by insoluble surfactants, come into contact and a coalescence event can be observed or not depending on the applied shear rate. Coalescence occurs at a critical capillary number resulting from a competition between the interaction time and the spontaneous drainage time. The droplets are close to each other during a given time, which depends on the shear rate and which can be compared to the time necessary to drain the liquid separating the droplets. At low shear rate, an effect of surfactant coverage attributed to the Marangoni stress on the surface has been demonstrated to limit the drainage. It appears that the inhibition of coalescence is maximized when the surface coverage reaches 30%. At larger shear rate, the viscous stress due to the Marangoni effect is no longer relevant; the drainage time is inertial so the coalescence time is highly reduced. These effects are well supported by numerical simulations taking into account diffusion and convection of surfactants along the interface.[54] A similar mechanism and, in particular, the effect of Marangoni stress on drainage at intermediate velocity has been proposed in an experiment in a thin-film pressure balance for saturated salt solutions of water.[55]

2. Surfactant depletion and coalescence induced by elongation: Experiments in micro channels show that coalescence is generally induced when bubbles are pulled apart, due to the formation of a nipple in a local zone in which surfactants are depleted (Figure 10A).[57]
3. Coalescence induced by topological transitions: Biance et al. (Figure 10B)[56] performed experiments concerning the coalescence of two bubbles during a topological transition. In this case, the bubbles consist of gas surrounded by a liquid shell. The bubbles are put in contact, leading to the merging of the films, then the coalescence of the two gas capsules is investigated. It was shown that coalescence is critically dependent on the quantity of liquid present at the beginning of the contact process. This critical amount of liquid itself depends greatly on the type of surfactant. A mechanism based on the observation that the freshly formed film is thicker than the initial film because its thickness is governed by hydrodynamics is proposed. Coalescence is likely to happen if the quantity of liquid available is smaller than the volume necessary for film formation. Although orders of magnitude are acceptable, this mechanism is lacking a proper description of film formation during the contact process.

Finally, all these experiments at the scale of a few bubbles show that local mechanical deformations that may occur in a foam can lead to bubble coalescence; thus, foam flow as well as foam aging can entrain foam coalescence due to dynamic events.

3.2.2. 2D Foams

To go to larger scale systems, experiments were performed in 2D foams.[58–60] A first experiment involved shearing of a foam in a Couette cell.[58] Coalescence occurs above a prescribed shear rate, in good agreement with experiments performed at the scale of two bubbles. However, this critical shear rate is reported to depend on the bubble radius, which shows that the mechanism proposed is different.[52,53] Indeed, Leal et al. show that shearing 2D foams not only increases the forces between approaching bubbles but also tends to create some liquid fraction inhomogeneities in the foam by centripetal forces. Then, the main factor inducing coalescence could be either a critical liquid fraction or an imposed shear. This experiment does not allow the two processes to be discriminated.

Coalescence was also studied in a bubble raft at the top of a liquid tank.[59] In this experiment, Ritacco et al. show propagation of coalescence events similar to avalanches when a first rupture is initiated. Such avalanches are reported to be inhibited by the presence of a larger viscous continuous phase.

In the case of deformation, the characteristic timescale of the coalescence process is externally imposed by the deformation rate. One may wonder whether this time is larger than the spontaneous rupture or not. In particular, if it is much shorter, the rupture may be induced before reaching the scenarios described in Section 2.2.2.3 (film thinning and hole initiation).

In the case of propagation of rupture events, the characteristic timescale will be the propagation time of the structural rearrangements within the foam. Then the dynamic of bubble rearrangements multiplied by the number N of rupturing bubbles defines the timescale for foam collapse. This leads to a timescale $t_a = N\kappa/\gamma$,[61,62] where κ is the surface viscosity. Taking $\kappa \simeq 0.1$ MPa m s for mobile interfaces and $\kappa \simeq 30$ MPa m s for rigid interfaces, we can calculate the time for 100 bubbles to burst: $t_a = 0.29$ s for mobile interfaces and $t_a = 85$ s for rigid interfaces. Note that the bulk viscosity does not appear in this calculation. Thus, it does not explain the inhibition of avalanches in the presence of a viscous continuous phase.

To conclude, experiments at the scale of a foam film or of a few bubbles show that mechanical deformations can induce coalescence due to interface deformation coupled to surfactant depletion. The exact mechanism is then highly dependent on the mechanical deformation.

4. Stability in Liquid Foams

The bridge between the stability of a few bubbles and of a 2D foam on the one hand and a macroscopic 3D foam on the other hand has not yet been established. As we will see in the following section, several experiments have been performed to identify the mechanisms leading to foam collapse, but often many parameters are tuned simultaneously and, despite the large amount of work on the subject, no clear picture has been proposed so far. We can distinguish the effect of foam structure and the effect of surfactant types used for stability.

4.1. Physical Parameters Governing Foam Collapse

Concerning the relevancy of physical mechanisms during foam destabilization, two different scenarios are proposed. The first is a spontaneous process in which films rupture at rest due to a strong pressure gradient leading to film drainage and rupture.[63–65] The second is a dynamic process that is more in line with the results of experiments at the scale of a film or few bubbles (Section 3) and correlates mechanical deformations in the foam with the coalescence process and collapse.[56,66] In this second picture, the dynamic is crucial to describe foam coalescence.

By following these two complementary analyses of foam collapse and noting that dry foams are less stable than wet foams, two main mechanisms are proposed in the literature. In the first, coalescence is suggested to be triggered by a critical capillary pressure because a film is unable to sustain a pressure larger than the local maximum of the disjoining pressure (Figure 4), as observed in isolated thin film experiments.[29,64,67,68] In the second, foam stability is governed by a critical liquid fraction because a minimum quantity of liquid is necessary to allow dynamic events. In the following, we gather experiments on 3D foams in favor of each mechanism.

4.1.1. Existence of a Critical Capillary Pressure

In an attempt to extend the results obtained at the scale of a film to foam stability, different studies have compared the maximum pressure that can be applied to a foam to the maximum of the disjoining pressure observed in similar foam films. In particular, two sets of experiments performed in foams and emulsions tend to show that coalescence is driven by a critical capillary pressure. Bibette et al.[63] looked at emulsions put under pressure as a result of osmotic stress induced through a dialysis membrane. They measured the critical external pressure Π_c at which coalescence occurs and observed a dependence on the droplet radius. The capillary pressure endorsed by the films can be related to this external pressure by the relation $\Pi_c = P_c - \frac{2\gamma}{R_v} = \frac{\gamma}{r_c} - \frac{2\gamma}{R_v}$. If coalescence occurs at a critical capillary pressure γ/r_c, a linear variation of Π_c with $1/R_v$ is then expected, which is indeed observed experimentally. Khristov et al.[64] performed similar experiments on foams and also observed coalescence at a critical pressure Π_c. Their main observations were that 1) for a certain type of surfactant, Π_c in foams is equal to the critical pressure that a similar foam film can sustain ($\Pi_c \propto 1/R_v$), and that 2) for another type of surfactants, Π_c, in this case, decreases when the bubble/film radius increases. These two different behaviors suggest the role of surfactants in coalescence mechanisms. Moreover, in another study,[69] the discrepancy between foam film and macroscopic foam critical pressure is more pronounced and is shown to depend on the details of the surfactant chemistry (hydrophobic chain length for example). These observations are in line with a stochastic film rupture in foams (scenario 2) because overcoming the maximum disjoining pressure should lead to NBFs, which must destabilize through the development of an instability. As mentioned above, Khristov et al. report another type of behavior for SDS/NaCl surfactant mixtures, in which a discrepancy is observed between the maximal pressure that can be sustained by an isolated film or by an entire foam. They attribute this effect to the polydispersity of the foam because the collapse is governed by the larger films, but they did not check this conclusion experimentally.

These two studies show that the rupture of films in a foam or an emulsion can be tuned by a critical capillary pressure. This mechanism should lead, in some cases, to foam collapse after a given drainage time due to the increase of capillary pressure under foam drainage.

4.1.2. Existence of a Critical Liquid Fraction

Other studies point to the role of mechanically driven foam collapse and, in particular, show that a foam collapses at a critical liquid fraction. In the first set,[66] the foam experiences forced drainage so that a given liquid fraction can be imposed uniformly over the foam. In a second set of experiments,[56] foams were submitted to a local mechanical deformation to induce local rearrangements. Biance et al. showed that collapse occurs at a prescribed liquid fraction, comparable in both studies, which depends very slightly on the bubble size over one order of magnitude. In the first experiment, they also show that this critical liquid fraction slightly depends on the surfactant concentration. The capillary pressure is then calculated and appears to be too small to explain foam collapse because it is several orders of magnitude smaller than the pressure that a single film can sustain.

4.1.3. Why Do Foams Collapse?

Finally, each mechanism (isolated rupture of films or dynamic events) is supported by at least two sets of experiments, with a systematic variation of the bubble size. However, although the arguments in favor of a critical pressure sustained by each film of the foam are well understood, what fixes a critical liquid fraction and how dynamic events induce foam collapse remains badly understood. Both mechanisms lead to a deterministic time at which the foam will collapse: this time is fixed by the drainage time. We can also report experiments in dense monodisperse emulsions.[70] Deminiere et al. report variation of bubble size versus time, which scales as $1/\sqrt{(t)}$. This behavior is in good agreement with a coalescence rate proportional to droplet area, in favor of a stochastic process of film rupture. This analysis however ignores the role of pressure in coalescence rate, because when bubble size is varied, the disjoining pressure is also varied and this should affect the coalescence rate. A last study suggests that it is not the capillary pressure or the liquid fraction that governs coalescence but the bubble size.[71] However, once again, parameters have not yet been varied independently to discriminate these aspects.

To conclude, it should be mentioned that the two proposed mechanisms have been observed experimentally by Khristov et al.[64] and depend on surfactant type. Determining the parameter that fixes the limit between these two mechanisms remains an important challenge, with bubble size and surfactant chemistry being good candidates. As we will see in Section 4.2, it is also crucial to point out the role of the physical chemistry.

4.2. Physicochemical Aspects: Is Foam Coalescence Correlated to Interfacial Viscoelasticity?

As shown for the stability of an isolated foam film, the surface viscoelasticity should come into play to explain the stability of foams. Indeed this parameter not only fixes the boundary condition at the air/liquid interface and the draining time but also has an influence on the development of instabilities leading to the rupture of the films and can prevent the crossing of the disjoining pressure barrier. These are the theoretical assertions that gave rise to dozens of studies that have tried to correlate foam stability and surface rheology.[25,29,36,71–84]

Already at the scale of a single film, it is difficult to make a proper correlation. Nevertheless, it is often observed that, for a given family of surfactants, the longer the carbon chain, the better the film stability and the larger the surface viscoelasticity.[25,29] Furthermore, in many studies in Thin Film Pressure Balance, a qualitative correlation between surface dilational elasticity and foam films stability is found.[25,36,72]

At the scale of the foam, many studies have been performed but it is difficult to answer clearly whether there is a correlation between foam stability and surface rheology.

The first difficulty is that the definition and the measurement of foam stability varies from one article to another. It can be the volume of air which can be incorporated in a foam,[76,77] the half-life time of a foam,[71,73] the time spent by a bubble in the foam before reaching the top,[79,80] the height of foam generated at a given flow rate,[74,75] or the appearance of a clear liquid/air interface.[78] Note that these methods measure either what we could call the foamability of a solution or the stability of a foam made with a given solution. Both definitions make sense because coalescence should appear in both cases; however, they are not comparable. Moreover, even if the method used to create a foam is the same, there is no guarantee that changing the stabilizer or its concentration will not change the bubble size or the volume fraction, which are both expected to be crucial parameters in foam coalescence.

The second difficulty is that the parameter chosen to represent the surface viscoelasticity varies from one reference to another. Depending on the study, either the real or the imaginary part of the dilatational or shear modulus is chosen. The best parameter is certainly a combination of all of these.

These difficulties have been reported many times[71,74,75,78] and it can be concluded from these reports that, for a given formulation, a correlation between foam stability and surface rheology seems to exist with varying stabilizer concentrations. However, there is no collapse of the data when plotting the foam stability as a function of the surface viscoelasticity. A representative curve (Figure 11) of this result is extracted from the report by Wang and Yoon.[78]

This shows that if the surface viscoelasticity is a relevant parameter to describe foam stability, it is not the only one, which makes it very difficult the seek an experimental proof. Additional parameters such as the adsorption time of the surfactants at the interface, can also be very important, at least for the foamability.[73,85,86] If surfactants do not have time to reach the interface during the foaming time, they clearly have no chance to stabilize the bubbles. Moreover, as underlined before, these parameters can also affect drainage time or fluctuation development. A last parameter that appears to be crucial is naturally surfactant concentration, the more surfactant present, the more stable the foam.[66,87]

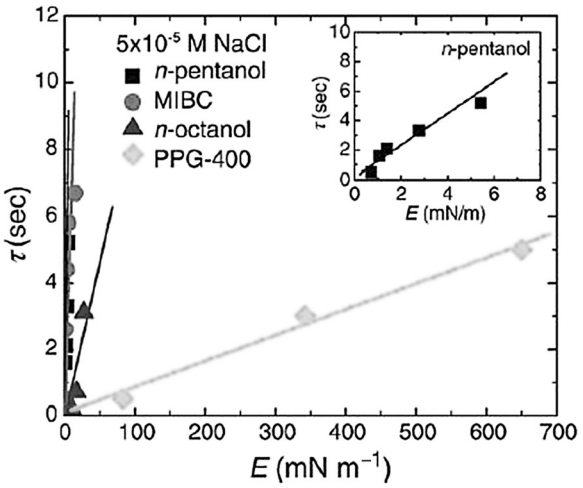

Figure 11. Reprinted with permission from Ref. [78]. Copyright 2008 Elsevier. The lifetime of a foam is shown as a function of the surface Gibbs elasticity calculated from the Langmuir isotherms. There is a correlation for each system but no collapse of the data.

4.3. Comparison of the Different Timescales

Different mechanisms are at the origin of coalescence in liquid foams, mainly spontaneous or triggered film rupture. Let us mention that for each mechanism, a macroscopic drainage of the foam is a prerequisite. All the proposed mechanisms rely on physical factors of a liquid foam. However, to discriminate in which case one predominates over the other, the different timescales involved in their development must be evaluated.

4.3.1. Timescale of Foam Drainage[88]

To obtain a typical timescale of foam drainage, we considered both limits of rigid and mobile interfaces. The drainage equation has been written within the lubrication hypothesis by two different groups, in the rigid limit[89,90] and in both limits.[91,92] The dimensionless drainage equation leads to a characteristic time t_0, a characteristic liquid fraction Φ_0 and a characteristic length z_0 which are different for rigid and mobile boundary conditions and which depend on the different geometrical parameters of the foam. In both cases, the volume fraction Φ versus the vertical position z in the foam evolves with time at a dimensionless velocity v, which is proportional to $\varepsilon = \frac{\Phi}{\Phi_0}$ in the rigid limit and $\sqrt{\varepsilon}$ in the mobile limit, respectively. Using the characteristic parameters for the velocity and considering a total height of foam $H = 30$ cm, we can deduce a typical drainage time $\tau_{\text{drainage}} = \frac{t_0}{z_0}\frac{H}{v}$ of approximately 1 h 10 min in the mobile case and 3 h 40 min in the rigid one. This is very long, but the model foam we choose has very small bubble size (the radius is around 50 μm) and the drainage is expected to be slow in such foams.

4.3.2. Isolated Film Rupture Mechanism

As depicted above, film rupture takes place in three steps. A drainage step is followed by the development of an instability and by the opening of a hole in the film. The three timescales determined above are summarized in the two cases of rigid and mobile interfaces in Table 1.

4.3.3. Mechanical Rupture of the Foam through Avalanche Propagation

As mentioned above, propagation of rupture within the foam, triggered by topological events, is, for certain cases, also at the origin of foam collapse. For mobile interfaces, this timescale is estimated to be approximately 0.3 s, and 85 s for rigid interfaces. In the case of mobile interfaces, this is the largest timescale after the foam drainage, so is perhaps a limiting factor.

5. Conclusion

We have shown that, we can compare the different relevant timescales of foam evolution (Table 2). It appears that hole nucleation as well as film drainage have negligible timescales. The avalanche seems to be an important mechanism, but it is also fast. Finally, the lifetime of a foam will be essentially set by the foam drainage. The timescale for the development of instabilities or the frequency of dynamic events can also be important depending on the rigidity of the interface and the underlying mechanism. In both cases, knowing the surface rheology of the interfaces as well as its exact impact on the drainage, the development of instabilities, and the frequency of dynamic events is crucial to predict the lifetime of a foam. If an external time is imposed, for example by shearing, it may control the entire dynamic.[93] Note that an important period, which is the coarsening time, is missing in this table. Obtaining a characteristic time for coarsening is actually still an open question. A foam that coarsens with very few coalescence events can indeed last between hours and months depending on the physical chemistry.[94] The extraction of such a characteristic timescale is, thus, beyond the scope of this Review. Therefore, the conclusion we can draw only concerns foams with lifetimes that are limited by coalescence.

We have seen that coalescence in liquid foams is a complex issue, mainly because of the multiscale structure of the foam.

Table 2. Timescales at play during foam coalescence. The parameters used in the calculation are the following: the initial thickness of the film is $h \simeq 1$ μm and its typical radius (close to the bubble radius) is $R_v \simeq 50$ μm. The PBs have a radius of curvature of $r = 6$ μm, which corresponds to a liquid fraction of 0.5%. The surfactant solution is an aqueous surfactant solution of viscosity $\eta = 10^{-3}$ Pa s, density $\rho = 1000$ kg m^{-3}, and surface tension $\gamma = 35$ mN m^{-1}.

Interfacial	Foam drainage	Film drainage	instability development	hole initiation	hole opening	Avalanches
rigid	220 min	8–80 μs	> 1 year	300 ms	2 μs	85 s
mobile	70 min	0.7 μs	280 μs	300 ms	2 μs	0.3 s

As for drainage, the physicochemistry of surfactants used is a crucial parameter that not only modifies the timescale of foam collapse, but also influences the precise mechanism inducing film rupture. Therefore, these parameters have a crucial role to play in the design of a stable foam. The coupling of the different mechanisms reviewed here and their coupling in real foams, in particular with defined structure (polydispersity) and complex physical chemistry, still requires extensive study. In particular, the role of dynamic events in film rupture remains little explored, and deserves an adequate study.

We would like to emphasize that a model foam was used to make all the calculations, so the timescales calculated here can change significantly depending on the geometry of the foam. For example, at a fixed liquid fraction, the bubble size mainly impacts the drainage of the whole foam. For example, if we take a foam with much larger bubbles, the drainage of the foam will be much smaller: approximately 5 min for mobile interfaces and 15 min for rigid interfaces. The liquid fraction also impacts the drainage of the films. If we choose a much wetter foam, let us say $\Phi = 4\%$, for example, we find very different values for the drainage of a single film (200 μs in the mobile case and 1 μs in the rigid case) and of the whole foam (45 min in the mobile limit and 90 min in the rigid limit). To compare to the other timescales, the numbers concerning drainage of foam films and of foams should be replaced by those in Table 2. This shows that in future experiments it will be important to control and vary the bubble size. Moreover, the importance of physicochemical parameters, such as the surface rheology, has been demonstrated. However, this also shows that it is crucial to choose a common definition for foamability and stability of a foam. For the foamability, we propose to take the volume of foam created by bubbling into a soapy solution at a given flow rate and with a controlled bubble radius. For the foam stability, we suggest to choose the time at which a catastrophic collapse event is observed.

Acknowledgements

A.-L. B. would like to thank Oriane Bonhomme, Bernard Cabane, Pauline Petit and Olivier Pitois for fruitful discussions. E. R. is grateful to Dominique Langevin and Wiebke Drenckhan for careful reading and to Anniina Salonen for fruitful discussions.

Keywords: liquids · materials science · membranes · surfactants · thin films

[1] P. Stevenson, *Foam engineering: fundamentals and applications*, Wiley-VCH, Weinheim, **2012**.
[2] E. Lorenceau, N. Louvet, F. Rouyer, O. Pitois, *Eur. Phys. J. E* **2009**, *28*, 293.
[3] V. Carrier, S. Destouesse, A. Colin, *Phys. Rev. E* **2002**, *65*, 061404.
[4] A. Bhakta, E. Ruckenstein, *Adv. Colloid Interface Sci.* **1997**, *70*, 1.
[5] A. Colin in *Foam Engineering* (Ed.: P. Stevenson), Wiley-VCH, Weinheim, **2012**, pp. 75 – 90.
[6] E. Rio, D. Langevin in *Encyclopedia of Surface and Colloid Science* (Ed.: P. Somasundaran), Taylor and Francis, New York, **2012**.
[7] V. A. Scheludko, *Colloid Polym. Sci.* **1957**, *155*, 39.
[8] K. J. Mysels, K. Shinoda, S. Frankel, *Soap Films: Studies of their thinning, Vol. 1*, Pergamon, Oxford, **1959**.
[9] I. Cantat, B. Dollet, *Soft Matter* **2012**, *8*, 7790.
[10] E. A. van Nierop, B. Scheid, H. A. Stone, *J. Fluid Mech.* **2008**, *602*, 119.
[11] B. Scheid, S. Dorbolo, L. R. Arriaga, E. Rio, *Phys. Rev. Lett.* **2012**, *109*, 264502.
[12] A. W. Adamson, A. P. Gast, *Physical Chemistry of Surfaces*, Wiley-VCH, Weinheim, **1997**.
[13] J. Lucassen, R. S. Hansen, *J. Colloid Interface Sci.* **1967**, *23*, 319.
[14] L. Landau, E. Lifshitz. *Fluid Mechanics*, Pergamon, Oxford, **1959**.
[15] A. A. Sonin, A. Bonfillon, D. Langevin, *J. Colloid Interface Sci.* **1994**, *162*, 323.
[16] A. Aradian, E. Raphaël, P. G. de Gennes, *Europhys. Lett.* **2001**, *55*, 834.
[17] P. D. Howell, H. A. Stone, *Eur. J. Appl. Math.* **2005**, *16*, 569.
[18] R. R. Dagastine, G. W. Stevens, D. Y. C. Chan, F. Grieser, *J. Colloid Interface Sci.* **2004**, *273*, 339.
[19] O. Manor, D. Y. C. Chan, *Langmuir* **2010**, *26*, 655.
[20] L. W. Schwartz, R. V. Roy, *J. Colloid Interface Sci.* **1999**, *218*, 309.
[21] D. Exerowa, D. Kashchiev, D. Platikanov, *Adv. Colloid Interface Sci.* **1992**, *40*, 201.
[22] J. K. Angarska, B. S. Dimitrova, K. D. Danov, P. A. Kralchevsky, K. P. Ananthapadmanabhan, A. Lips, *Langmuir* **2004**, *20*, 1799.
[23] D. S. Valkovska, K. D. Danov, I. B. Ivanov, *Adv. Colloid Interface Sci.* **2002**, *96*, 101.
[24] J. Israelachvili, *Intermolecular and Surface Forces*, 3edrd edAcademic Press, San Diego, **2010**.
[25] C. Stubenrauch, R. von Klitzing, *J. Phys. Condens. Matter* **2003**, *15*, R1197.
[26] V. Bergeron, D. Langevin, A. Asnacios, *Langmuir* **1996**, *12*, 1550.
[27] A. Asnacios, A. Espert, A. Colin, D. Langevin, *Phys. Rev. Lett.* **1997**, *78*, 4974.
[28] K. J. Mysels, M. N. Jones, *Discuss. Faraday Soc.* **1966**, *42*, 42.
[29] V. Bergeron, *Langmuir* **1997**, *13*, 3474.
[30] G. I. Taylor, *Proc. R. Soc. London Ser. A* **1959**, *253*, 313.
[31] A. J. de Vries, *Recl. Trav. Chim. Pays-Bas* **1958**, *77*, 383.
[32] A. Vrij, *J. Colloid Sci.* **1964**, *19*, 1.
[33] A. Vrij, J. T. G. Overbeek, *J. Am. Chem. Soc.* **1968**, *90*, 3074 – 3078.
[34] A. Vrij, *Discuss. Faraday Soc.* **1966**, *42*, 23.
[35] H. Wennerström, J. Morris, U. Olsson, *Langmuir* **1997**, *13*, 6972.
[36] E. Santini, F. Ravera, M. Ferrari, C. Stubenrauch, A. Makievski, J. Kragel, *Colloids Surf. A* **2007**, *298*, 12.
[37] P. G. de Gennes, *Chem. Eng. Sci.* **2001**, *56*, 5449.
[38] P. G. de Gennes, *Langmuir* **2001**, *17*, 2416.
[39] K. Khristov, D. Exerowa, P. M. Kruglyakov, *Colloids Surf. A* **1993**, *78*, 221.
[40] E. D. Manev, A. V. Nguyen, *Adv. Colloid Interface Sci.* **2005**, *114 – 115*, 133.
[41] F. E. C. Culick, *J. Appl. Phys.* **1960**, *31*, 1128.
[42] W. R. McEntee, K. J. Mysels, *J. Phys. Chem.* **1969**, *73*, 3018.
[43] S. Frankel, K. J. Mysels, *J. Phys. Chem.* **1969**, *73*, 3028.
[44] N. Y. Liang, C. K. Chan, H. J. Choi, *Phys. Rev. E* **1996**, *54*, R3117.
[45] L. J. Evers, S. Y. Shulepov, G. Frens, *Phys. Rev. Lett.* **1997**, *79*, 4850.
[46] P. G. de Gennes, F. Brochard-Wyart, D. Quéré, M. Fermigier, C. Clanet, *Gouttes, bulles, perles et ondes*, Belin, **2002**.
[47] G. Debregeas, P. G. de Gennes, F. Brochard-Wyart, *Science* **1998**, *279*, 1704.
[48] *Anionic surfactants: physical chemistry of surfactant action* (Ed.: J. Lucassen), Marcel Dekker, New York, **1981**.
[49] C. J. W. Breward, P. D. Howell, *J. Fluid Mech.* **2002**, *458*, 379.
[50] L. Saulnier, F. Restagno, J. Delacotte, D. Langevin, E. Rio, *Langmuir* **2011**, *27*, 13406.
[51] L. Saulnier, L. Champougny, G. Bastien, F. Restagno, D. Langevin, E. Rio, *Soft Matter* **2014**, *10*, 2899 – 2906.
[52] L. G. Leal, *Phys. Fluids* **2004**, *16*, 1833.
[53] Y. Yoon, A. Hsu, L. G. Leal, *Phys. Fluids* **2007**, *19*, 023102.
[54] C. Vannozzi, *Phys. Fluids* **2012**, *24*, 082101.
[55] V. V. Yaminsky, S. Ohnishi, E. A. Vogler, R. G. Horn, *Langmuir* **2010**, *26*, 8061.
[56] A. L. Biance, A. Delbos, O. Pitois, *Phys. Rev. Lett.* **2011**, *106*, 068301.
[57] N. Bremond, A. R. Thiam, J. Bibette, *Phys. Rev. Lett.* **2008**, *100*, 024501.
[58] H. Mohammadigoushki, G. Ghigliotti, J. J. Feng, *Phys. Rev. E* **2012**, *85*, 066301.
[59] H. Ritacco, F. Kiefer, D. Langevin, *Phys. Rev. Lett.* **2007**, *98*, 244501.
[60] I. Ben Salem, I. Cantat, B. Dollet, *J. Fluid Mech.* **2013**, *714*, 258.
[61] M. Durand, H. A. Stone, *Phys. Rev. Lett.* **2006**, *97*, 226101.

[62] A. L. Biance, S. Cohen-Addad, R. Hoehler, *Soft Matter* **2009**, *5*, 4672.
[63] J. Bibette, D. C. Morse, T. A. Witten, D. A. Weitz, *Phys. Rev. Lett.* **1992**, *69*, 2439.
[64] K. Khristov, D. Exerowa, G. Minkov, *Colloids Surf. A* **2002**, *210*, 159.
[65] N. G. Vilkova, P. M. Kruglyakov, *Adv. Colloid Interface Sci.* **2004**, *108*, 159.
[66] V. Carrier, A. Colin, *Langmuir* **2003**, *19*, 4535.
[67] D. Exerowa, A. Nikolov, M. Zacharieva, *J. Colloid Interface Sci.* **1981**, *81*, 419.
[68] D. Exerowa, T. Kolarov, K. H. R. Khristov, *Colloids Surf.* **1987**, *22*, 161.
[69] C. Stubenrauch, V. B. Fainerman, E. V. Aksenenko, R. Miller, *J. Phys. Chem. B* **2005**, *109*, 1505.
[70] B. Deminiere, A. Colin, F. Leal-Calderon, J. F. Muzy, J. Bibette, *Phys. Rev. Lett.* **1999**, *82*, 229.
[71] D. Georgieva, A. Cagna, D. Langevin, *Soft Matter* **2009**, *5*, 2063.
[72] C. Stubenrauch, R. Miller, *J. Phys. Chem. B* **2004**, *108*, 6412.
[73] A. Pinazo, L. Perez, M. R. Infante, E. I. Franses, *Colloids Surf. A* **2001**, *189*, 225.
[74] A. Bhattacharyya, F. Monroy, D. Langevin, J. F. Argillier, *Langmuir* **2000**, *16*, 8727.
[75] C. Monteux, G. G. Fuller, V. Bergeron, *J. Phys. Chem. B* **2004**, *108*, 16473.
[76] H. Fruhner, K. D. Wantke, K. Lunkenheimer, *Colloids Surf. A* **2000**, *162*, 193.
[77] S. Rouimi, C. Schorsch, C. Valentini, S. Vaslin, *Food Hydrocolloids* **2005**, *19*, 467.
[78] L. Wang, R. H. Yoon, *Int. J. Miner. Process.* **2008**, *85*, 101.
[79] K. Małysa, K. Lunkenheimer, R. Miller, C. Hempt, *Colloids Surfaces* **1985**, *16*, 9.
[80] K. Wantke, K. Malysa, K. Lunkenheimer, *Colloids Surf. A* **1994**, *82*, 183.
[81] P. J. Wilde, *Curr. Opin. Colloid Interface Sci.* **2000**, *5*, 176.
[82] D. Langevin, *Adv. Colloid Interface Sci.* **2000**, *88*, 209.
[83] M. Golding, A. Sein, *Food Hydrocolloids* **2004**, *18*, 451.
[84] S. Vandebril, J. Vermant, P. Moldenaers, *Soft Matter* **2010**, *6*, 3353.
[85] A. Salonen, M. In, J. Emile, A. Saint-Jalmes, *Soft Matter* **2010**, *6*, 2271.
[86] K. G. Marinova, E. S. Basheva, B. Nenova, M. Temelska, A. Y. Mirarefi, B. Campbell, I. B. Ivanov, *Food Hydrocolloids* **2009**, *23*, 1864.
[87] R. Mensire, K. Piroird, E. Lorenceau, *Soft Matter* **2014**, *10*, 7068.
[88] M. Durand, *Contributions théorique et expérimentale à l'étude du drainage d'une mousse liquide*. PhD thesis, Université Paris XI, **2000**.
[89] D. Weaire, S. Findlay, G. Verbist, *J. Phys. Condens. Matter* **1995**, *7*, L217.
[90] G. Verbist, D. Weaire, A. M. Kraynik, *J. Phys. Condens. Matter* **1996**, *8*, 3715.
[91] S. A. Koehler, S. Hilgenfeldt, H. A. Stone, *Phys. Rev. Lett.* **1999**, *82*, 4232.
[92] S. A. Koehler, S. Hilgenfeldt, H. A. Stone, *Langmuir* **2000**, *16*, 6327.
[93] K. Golemanov, S. Tcholakova, N. D. Denkov, K. P. Ananthapadmanabhan, A. Lips, *Phys. Rev. E* **2008**, *78*, 051405.
[94] A. Saint-Jalmes, M. L. Peugeot, H. Ferraz, D. Langevin, *Colloids Surf. A* **2005**, *263*, 219.
[95] I. U. Vakarelski, R. Manica, X. Tang, S. J. O'Shea, G. W. Stevens, F. Grieser, R. R. Dagastine, D. Y. C. Chan, *Proc. Natl. Acad. Sci. USA* **2010**, *107*, 11177.

Received: April 2, 2014
Revised: June 24, 2014
Published online on September 26, 2014